The Automated Solar Activity Prediction System (ASAP) Update Based on Optimization of a Machine Learning Approach

Ali K. Abed(✉) and Rami Qahwaji

Bradford University, Bradford, UK
{a.k.abed,r.s.r.qahwaji}@bradford.ac.uk

Abstract. Quite recently, considerable attention has been paid to solar flare prediction because extreme solar eruptions could affect our daily life activities and on different technologies. Therefore, this paper presents a novel method of the development of improved second-generation of the Automated Solar Activity Prediction system (ASAP). The suggested algorithm improves the ASAP system by expanding a period of training vector and generating new machine learning rules to be more successful. Two neural networks are responsible for determining whether the sunspots group will release flare as well as determining if the flare is an M-class or X-class. Several measurement criteria are applied to determine the extent of system performance also all results are provided in this paper. Furthermore, the quadratic score (QR) is used as a metric criterion to compare between the prediction of the proposed algorithm with the Space Weather Prediction Center (SWPC) between 2012 and 2013. The results exhibit that the proposed algorithm outperforms the old ASAP system. Keywords: Solar flares, Machine Learning, Neural network, Space, Prediction, weather.

Keywords: Neural networks · Automated Solar Activity Prediction · Sunspot · McIntosh classifications

1 Introduction

Nowadays, space weather prediction in real-time is an important issue for many countries because of extreme solar eruptions could influence our daily life activities and affect various technologies. Wherefore, the U.S. National Space Weather Program (NSWP) defined space weather as "conditions on the Sun and in the solar wind, magnetosphere, ionosphere, and thermosphere that can influence the performance and reliability of space-borne and ground-based technological systems and can endanger human life or health" [1]. Wherefore, the significance of studying space weather is increasing.

Solar flares and Coronal Mass Ejections (CMEs) are solar events that have a significant impact on daily life and on different technologies at Earth [2]. As a result, these solar activities can spew vast quantities of radiation and charged particles into space this causes extreme ultraviolet and X-ray flux from flares reacted with the ionosphere making widespread blackout situations for High-Frequency radio communications [3].

K. Arai et al. (Eds.): SAI 2020, AISC 1230, pp. 702–717, 2020.
https://doi.org/10.1007/978-3-030-52243-8_53

In spite of the fact that the event of these activities cannot be stopped. However, predicting when these solar activities are possible to occur could reduce possible damage to industries, for example, space agencies, power generation and distribution industry, oil, satellite operators and gas industry, and thus lead to a lowering in their economic effect. Solar flare study has confirmed that Solar flares and Coronal Mass Ejections (CMEs) are generally associated to active regions and sunspots [3–5].

There are predictive science researchers and different research organizations scattered all over the world are involving in solar prediction and analysis. These predictions usually rely mainly on experts with high knowledge in space weather, which may lead to a discrepancy in space weather forecasting. To solve these problems, objective computerized analysis of images surface of the sun can supply automated processing and consistent execution by applying the enormous computational abilities of computers with high-speed processing to analyse and compare huge amounts of new and historical data. Thus, there is still a need for design high-performance forecasting system.

There are many challenges facing the scientists of space weather forecasting. We can face those challenges by building an effective computer system has the ability to the automated determination, classification, and representation of solar features and the creation of a perfect correlation between these features and the appearance of solar activities. In order to propose an effective system for space weather forecasting, we need to apply real-time, high-quality space weather data and processing techniques to forecast solar activities (Wang et al. 2003). The launch new satellites for space weather, for example, the Solar Dynamics Observatory (SDO) has helped to provide accurate data this helped a solar events observation. Therefore, that requires prediction methods which conformity, and to benefit from, additional information in the data. Many predictions systems for instance, those depend on sunspot detection models, classification, machine learning algorithms, time-series analysis, and many more that have been suggested [6].

Previous studies indicate that there have been automated systems that can provide real-time forecasting of significant solar flares that may influence our Earth. The performance of the former automated systems that designed still will hope a better prediction than subjective analysis. For example, The University of Alabama in Huntsville developed new a technique called (MAG4) system of forecasting an active region's rate of production of greater flares in magnetic energy [7]. This system prediction depended on applying magnetogram data for the Sun. The principal work of this system is using the McIntosh active-region (AR) classes to prediction Solar Proton Events (SPE), CMEs, and M and X class flares.

Hong et al. [8] designed a system called Automatic Solar Synoptic Analyzer (ASSA) the main function of this system is identifying coronal holes, sunspot groups, and filament channels that are three properties responsible the space weather. This system is built depends on an artificial neural network technique with the ASSA coronal hole data archive of the period from 1997 to 2013. In addition, this system-applied image of SOHO EIT 195 and SDO AIA 193 used for morphological recognition and thereafter SOHO MDI Magnetograms and SDO HMI Magnetograms applied for quantitative verification. This system has the ability to predict three classes of solar flares are C, M, and X-flare.

We updated the Automated Solar Activity Prediction system (ASAP). It is an automated space weather forecasting system that contents from advanced image processing

and machine learning techniques with solar physics. The update process included the following steps: Increase the data used in the neural network training by increasing the time period. We have used the data from Dec 1918 to June 2017. In addition, a new training strategy was be used this paper. We will mention all the update details in the next part of this paper.

The remainder of the paper is organized as follows: Sect. 2 outlines the images processing method that is responsible for the automated detection and classification of sunspots. The machine learning models that are trained on solar flares and historical sunspot data are presented in Sect. 3; Sect. 4 discusses applying, integration, performance, and evaluation for Machine Learning system. The concluding and suggestions for future work are presented in Sect. 5 concludes the paper.

2 Detection and Classification for Sunspot

In 2008 Colak and Qahwaji [9] proposed a computer system that can automatically detect, group, and classify sunspots depend on the McIntosh classification. SDO/HMI Continuum and Magnetogram images use in this system as input to reveal sunspot regions and extract their features including their McIntosh classifications. In this study, this system working by integrated with a machine learning-based method to supply real-time forecasting for the probable occurrence of significant flares like type-X or type- M, as described in the next part in this report.

2.1 SDO HMI Images

The Solar Dynamics Observatory (SDO) supplies 13 various wavelengths of the sun. Two instruments have been used are the Helioseismic and Magnetic Imager (HMI) and the Atmospheric Imaging Assembly (AIA) instrument. In this study, we used two types of images are HMI Continuum and HMI Magnetogram. HMI Continuum provided images of the solar surface, incorporating a broad range of visible light for Solar Region Photosphere. On the other hand, HMI Magnetograms show maps of the magnetic field on the sun's surface, with black and white. the black showing magnetic field lines pointing away from Earth, On the contrary, the white showing magnetic field lines coming toward Earth for Solar Region Photosphere [10].

2.2 Sunspot Detection and Classification Algorithms in Colak and Qahwaji System

In this part of the report, we provide a brief about the worked algorithms of the system Colak and Qahwaji. These algorithms include different functions such as sunspot detection, grouping, and classification. The following steps for these algorithms:

1) **Pre-processing of HMI images**

- Continuum and magnetogram images used together to determine the solar disk, radius and centre, make a mask and remove any information for example date and direction from the image, calculate the Julian date and solar coordinates.

- Magnetogram images only use in this algorithm. Map the magnetogram image from Heliocentric-Cartesian coordinates to Carrington Heliographic coordinates. Centre, radius and solar coordinates of the continuum image use a replacement of centre, radius and solar coordinates of the magnetogram image of re-map to Heliocentric-Cartesian coordinate.

2) **Sunspot grouping**

- MDI continuum images using to detect sunspot candidates by applying limited intensity thresholding.
- MDI magnetogram images used to detect active region candidates by applying morphological image processing algorithms such as intensity filtering, dilation, and erosion.
- Use region growing approach to combine active region with sunspot candidates. More details about this technique are described in [9].
- Apply neural networks to combine regions of opposite polarities so as to determine the boundaries of sunspot groups.
- Sign the discovered sunspot groups.

3) **McIntosh-based Classification**

- Applying neural networks and image processing in order to detect local features from each sunspot in each group.
- Apply image processing in order to detect features from every sunspot group these features are largest spot, distribution, length, and polarity.
- Used a decision tree approach to determine McIntosh classification by used the extracted features as input for a decision tree.

3 Apply Machine Learning for Solar Flare Prediction

Many experts in space weather contend has shown that flares exceedingly related to active regions and sunspots [3–5]. A study of the solar physics literature characterizing the association between sunspots and flares was introduced in [11]. In this system, all information used as input to machine learning provided from historical data such as solar catalogues and converted it in computerized learning rules that allow computers system to analyse current solar data and supply solar flare forecasts.

3.1 Knowledge Representation of Solar Catalogues

The National Geophysical Data Centre (NGDC) provides sunspots groups catalogue and solar flares catalogue. These catalogues are publicly available on the (NGDC) website. The NGDC sunspot catalogue contains the following data the date, time, location, physical properties, and classification of sunspot groups, and the National Oceanic and Atmospheric Administration (NOAA) number, on the flip side, the NGDC flare catalogue contains the following data dates, starting and ending times for flare eruptions,

location, x-ray classification, and the National Oceanic and Atmospheric Administration (NOAA) number. The association is done through Atmospheric Administration (NOAA) number for the flare that is associated with the active region detected. In this section, a C++ platform created to automatically associate between sunspots and flares. NGDC has sunspot data from various observatories and sometimes contains different observations of the same sunspot group for various times of the same day. Flares and sunspot catalogues examined to associate sunspot groups with the solar flares, which are consider the main cause of these flares. All the recorded flares and sunspots for the periods from 1st December 1981 until 30th June 2017, which includes 71475 solar flares (43147 C-class, 5435 M-class and 417 X-class) and 271883 sunspot groups, are tested using the association algorithm described in [11].

The association algorithm is based on the following conditions:

- A sunspot and solar flare are associated if it has the same NOAA number. Whereas, sunspots and flares does not have NOAA numbers are filtered out from the lists.
- A solar flare catalogue should be listed after a sunspot within a predefined time window. Four-time windows were used: 6, 12, 24, and 48 h.
- If more than one sunspot associated with the same solar flare, only the nearest sunspot in time to the flare is considered as related, and the all remnant of sunspots are deleted.

Table 1. Illustrate the final association results for a sunspot and solar flare by the association algorithm.

Time window	C	M	X	Associated (A)	Not Associated (NA)	A + NA	Ignored
6	17210	2877	252	20339	53540	234,944	36,939
12	21615	3686	316	25617	24162	49779	185165
24	20011	3558	313	23882	8290	32172	224554
48	20234	3583	318	24135	3878	28013	228713

Table 1 represents the final association results between flare and sunspot for the periods from 1st December 1981 until 30th June 2017.

3.2 The Flare Prediction System

We applied the area of sunspot groups together with the McIntosh classes as the input for solar flare forecast algorithm in order to produce forecasts for the M-class and X-class flares. Our solar flare forecast algorithm is composed of two Neural Network (NN) illustrated in Fig. 1. McIntosh classifications and sunspot numbers for everyday applied as input to the neural network algorithms. Furthermore, we used tools like the Jack-knife method [12] to evaluate the training and generalization efficacies of the neural network algorithms. The first NN accepts four inputs. These inputs are the three McIntosh classes

and the sunspot area. On the other hand, this neural network provides one output in the range of 0.1 to 0.9 in the next 6, 12, 24 and 48 h and a threshold of 0.5 is used to categorize the generated outputs as 0.9 if >0.5 or 0.1 if <0.5, which represents flare or no-flare respectively. It produces the probability that this sunspot group will produce a solar flare in the next 6, 12, 24 and 48 h. Therefore, this first NN is trained using sunspot regions from the NGDC sunspot catalogue and solar flare from the NGDC flare catalogue associations as described in the previous section. The training vector includes four inputs numerical values and their corresponding single output value (Flare = 0.9 or No Flare = 0.1) as shown in Table 2. For instance, if there is a sunspot region with a McIntosh classification of EFI and an area of 875 in millionths of solar hemisphere that is related with solar flare then the training vector will be [0.7, 0.9, 0.5, 0.35; 0.9].

Table 2. Illustrate numerical values for the first neural network representing the McIntosh classes and sunspot area as the inputs and their corresponding target.

Inputs				Output
McIntosh classes			Normalized (with 2500) sunspot area	Flare= 0.9 No flare = 0.1
A = 0.10 H = 0.15 B = 0.20 C = 0.35 D = 0.60 E = 0.75 F = 0.90	X = 0 R = 0.10 S = 0.30 A = 0.50 H = 0.70 K = 0.90	X = 0 O = 0.10 I = 0.50 C = 0.90		

The second NN is worked to determine the forecasted flare is going to be M-class and/or X-class flare. The second NN trained using a training set that includes only the three McIntosh classes for sunspot groups that related to M-class and X-class flares. Therefore, the second NN includes three inputs and two outputs. The first and second outputs represent the M-class and X-class flares, respectively. This neural network works as follows:

- If the sunspot group is related only with an M-class flare, then the first output will be more than or equal to 0.5 otherwise it will be less than 0.5.
- If the sunspot group is related only with an X-class flare, then the second output will less than or equal to 0.5 otherwise it will be less than 0.5.
- If the sunspot group is related to M-class and X-class of a solar flare, all the corresponding outputs will be greater than or equal to 0.5 otherwise it will be less than 0.5.

For instance, if there is a McIntosh classification of FKI that is related only with M-class and X-class solar flares during the same time then the training vector for this example will be [0.9, 0.9, 0.5; 0.77, 0.56].

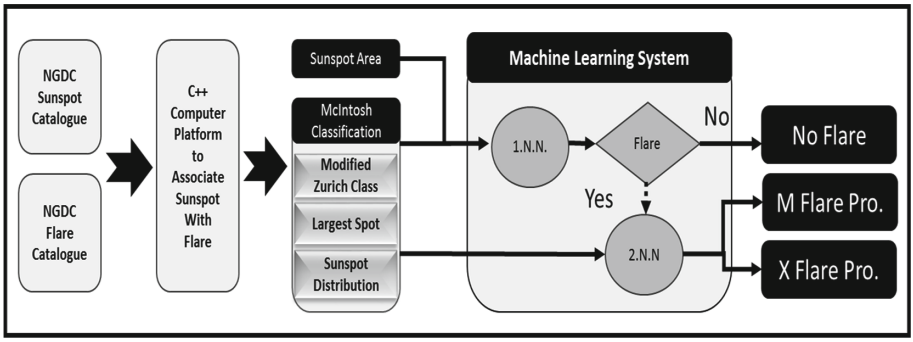

Fig. 1. Solar flare prediction algorithm with training and testing data.

3.3 Optimization of the Neutral Networks

The two neural networks are optimized by comparing the forecast outputs from the two neural networks against the actual outputs. From the comparison, the following measures are calculated first: True Positive (TP), False Positive (FP), True Negative (TN), and False Negative (FN). For this report, the significance of these measures is described in this section below:

- TP represents the number of cases when a sunspot group is related with an actual flare and a flare forecast is produced then this prediction is true.
- FP represents the number of cases when a sunspot group is related with an actual flare, but no flare forecast is produced then this prediction is wrong.
- TN represents the number of cases when a sunspot group is not related with any actual flare and no flare forecast is produced then this prediction is true.
- FN represents the number of cases when a sunspot group is not related with any actual flare, but no flare forecast is produced then this prediction is wrong.

We are using the measures above to calculating the prediction performance of the learning algorithm. These forecasting measures are:

- True Positive Rate (TPR), represents the possibility sunspot group finds that are successfully forecasted as flaring. Higher TPR represents a better prediction performance. This value is calculated by applying Eq. (1).

$$TPR = \frac{TP}{TP + FN} \tag{1}$$

- False Positive Rate (FPR), represents the possibility sunspot group finds that are unsuccessfully forecasted as flaring. Minimum FPR represents better prediction performance. This value is calculated by applying Eq. (2).

$$FPR = \frac{FP}{FP + TN} \tag{2}$$

- True Negative Rate (TNR), represents the possibility of non-flaring sunspots group finds that are unsuccessfully forecasted as non-flaring. Maximum TNR represents a better prediction performance. This value is calculated by applying Eq. (3).

$$TNP = \frac{TN}{FP + TN} \tag{3}$$

- False Negative Rate (FNR), represents the possibility of flaring sunspot group finds that are unsuccessfully forecasted as non-flaring. Minimum FNR represents better prediction performance. This value is calculated by applying Eq. (4).

$$FNP = \frac{FN}{TP + FN} \tag{4}$$

- False Alarm Rate (FAR), represents the possibility of false flare forecasts. Minimum FAR represents better prediction performance. This value is calculated using Eq. (5).

$$FAR = \frac{FP}{FP + TP} \tag{5}$$

- Mean Squared Error (MSE), this value represents the average of the squares of the difference between the predicted flare cases and the actual flare cases for all sunspot group detections. A minimum MSE value represents better prediction performance. This value is calculated by applying Eq. (6).

$$MSE = \frac{1}{n}\sum_{i=1}^{n}(p_i - r_i)^2 \tag{6}$$

Where, p_i is the value of all output for the inputs given in the training vector, and r_i is the actual output given in the training vector, n is the whole number of symbols in the training vector.

- Accuracy (ACC), this value represents how close the overall forecast produces are to the actual values. Maximum ACC rates represent a better prediction performance. This value is calculated by applying Eq. (7).

$$ACC = \frac{TR + TN}{(TP + FN) + (FP + TN)} \tag{7}$$

- Heidke Skill Score (HSS), this value represents the chance factor of predicting. The value of HSS is between −1 to 1. Negative values represent the prediction is based on chance, 0 shows no-skill, and positive values represent perfect forecasting.

$$HSS = \frac{2 \times ((TP \times TN) - (FP \times FN))}{((TP + FN) \times (FN + TN) + ((TP + FP) \times (FP + TN))} \tag{8}$$

More details on these measures can get from [13]. Several training experiments are carried out while changing the number of nodes in the hidden layer as follows.

3.4 Optimization Strategies

For each association time window (6, 12, 24, and 48), the training and testing methods for the first neural network was as follows:

- 10-time training experiments are carried out while changing the number of nodes in the hidden layer from 1 to 15.
- The average and standard deviation to the forecasting measures were calculated for different decision thresholds (0.5, 0.45, 0.4, and 0.35) and different time-window (6, 12, 24, and 48) for each experiment (Table 3).

Table 3. Shows the best number of nodes used in the hidden layer for the first neural network to different decision thresholds (0.5, 0.45, 0.4, and 0.35) and different time-window (6, 12, 24, and 48).

Threshold	Time window	Nodes	Run	TPR	FPR	FNR	TNR	FAR	ACC	SPC	HSS	MCC	TSS
0.35	6	6	Mean	0.4340	0.0218	0.5660	0.9782	0.4597	0.9481	0.9782	0.4526	0.4565	0.4121
0.45	12	9	Mean	0.6635	0.0506	0.3365	0.9494	0.3124	0.9090	0.9494	0.6207	0.6220	0.6128
0.35	24	3	Mean	0.8669	0.1105	0.1331	0.8895	0.2350	0.8828	0.8895	0.7277	0.7311	0.7564
0. 5	48	2	Mean	0.8705	0.0823	0.1295	0.9177	0.1020	0.8962	0.9177	0.7901	0.7906	0.7882

Four sets of decision rules for the neural network were created by retraining the full dataset of associations between sunspots and flares: flare_6.dat, flare_12.dat, flare_24.dat, and flare_48.dat.

For each association time window (6, 12, 24, and 48), the training and testing methods for the second neural network was handled as follows:

- The number of hidden nodes for the second neural network was varied from 1 to 20.
- The only one measure that used to measure the second neural network performance was the MSE.
- From the former table (Table 4), it was found the best neural network structure for the second neural network are: 20 hidden nodes for 6 h forecast window, 18 hidden nodes for 12 h forecast window, 19 hidden nodes for 24 h forecast window, and 20 hidden nodes for 48 h forecast window.
- Four sets of decision rules were created: intensity_6.dat, intensity_12.dat, intensity_24.dat, and intensity_48.dat.

Table 4. Shows the best number of nodes applied in the hidden layer for the second neural network to different time-window (6, 12, 24, and 48).

Time	MSE	Number of Hidden Nodes																			
		1	2	3	4	5	6	7	8	9	10	11	12	13	14	15	16	17	18	19	20
6	M	0.0234	0.0213	0.0213	0.0214	0.0214	0.0214	0.0314	0.0127	0.0079	0.0171	0.0068	0.0336	0.0117	0.0063	0.0039	0.0111	0.0037	0.0039	0.0064	0.0031
	X	0.0217	0.0206	0.0206	0.0206	0.0206	0.0206	0.0367	0.0180	0.0259	0.0204	0.0133	0.0332	0.0103	0.0128	0.0096	0.0181	0.0097	0.0067	0.0119	0.0068
12	M	0.0242	0.0242	0.0242	0.0242	0.0242	0.0242	0.0242	0.0242	0.0242	0.0242	0.0242	0.0242	0.0242	0.0242	0.0242	0.0242	0.0242	0.0242	0.0242	0.0242
	X	0.0174	0.0145	0.0168	0.0168	0.0168	0.0168	0.0145	0.0196	0.0159	0.0107	0.0160	0.0171	0.0171	0.0126	0.0064	0.0105	0.0108	0.0038	0.0082	0.0065
24	M	0.0239	0.0218	0.0218	0.0219	0.0218	0.0159	0.0186	0.0158	0.0070	0.0048	0.0223	0.0073	0.0143	0.0128	0.0046	0.0049	0.0050	0.0043	0.0035	0.0051
	X	0.0170	0.0159	0.0159	0.0159	0.0159	0.0167	0.0164	0.0173	0.0090	0.0065	0.0310	0.0077	0.0142	0.0154	0.0053	0.0072	0.0056	0.0066	0.0029	0.0090
48	M	0.0240	0.0216	0.0216	0.0216	0.0216	0.0121	0.0121	0.0149	0.0132	0.0275	0.0091	0.0219	0.0073	0.0059	0.0096	0.1734	0.0094	0.0054	0.0054	0.0052
	X	0.0178	0.0167	0.0167	0.0167	0.0167	0.0153	0.0092	0.0162	0.0297	0.0269	0.0091	0.0219	0.0082	0.0107	0.0117	0.3186	0.0188	0.0101	0.0118	0.0109

4 Actual Implementation and Evaluation of Updates ASAP's System

The main principles work of ASAP's system is integrating the imaging and machine learning systems for the hybrid solar flare forecast. This system is shown in Fig. 2. The inputs of this system are HIM images from SDO. The system starts its real-time working by deals with SDO/HIM continuum and magnetogram images in the method illustrated in Sect. 2 to issue automated McIntosh classifications for the detected sunspots group. After that, the McIntosh classified sunspots and sunspot area are fed to the machine learning system(first and second neural network) explained in Sect. 3 which is trained with 37 years of data after applying the association algorithm. Based on the embedded learning rules the system predicts if a solar flare is going to occur or not without time windows were used (6, 12, 24, and 48 h). If a significant solar flare is forecasted then the probability of this solar flare to be M-class or X-class flare is also predicted. The entire system is implemented in C++.

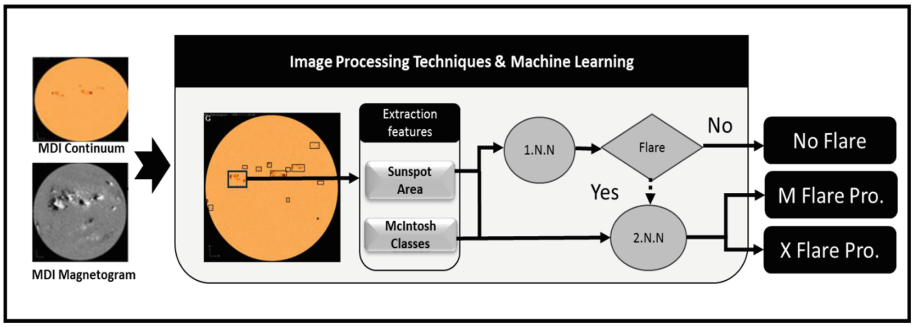

Fig. 2. The final updated ASAP system

4.1 Evaluation of the Updated ASAP System

The update ASAP's system was tested on solar SDO HMI continuum images from January 1, 2012, to December 31, 2013. Furthermore, the performance of the new system was evaluated by comparing the produced forecasts with the actual flares as registered by NOAA SWPC1 in the NGDC X-ray solar flare catalogue and with old ASAP. There were 67787 HIM continuum images available during this period at a cadence of 96 images per day. These HIM continuum images and their corresponding 67787 MDI magnetogram images were processed using the updated ASAP System and four sunspot catalogues was generated which we refer to as ASAPDATABASE_06, ASAPDATABASE_12, ASAPDATABASE_24, and ASAPDATABASE_48. Parts of the ASAPDATABASE_06.

With a view to linking the sunspot groups detected by our system together with x-ray solar flares registered in the NGDC catalogue, we had to update the association algorithm, suggested in (Qahwaji and Colak, 2007), the main details of this algorithm as follows:

- A special version of the association algorithm updated to find the associations between the sunspots reported by new ASAP system and the flares reported in the NGDC flares catalogues. These associations were found based on the availability of flare locations and the possibility of having a flare event within the used association time window (6, 12, 24, or 48 h).

  - Read all the sunspot groups and their solar flare forecast as written in ASAPDATABASE_06, ASAPDATABASE_12, ASAPDATABASE_24, and ASAPDATABASE_48 files.
  - Read all the actual M and X-class flares as written in the NGDC solar flare catalogue.

- Carry out an search to link all actual solar flare with its corresponding sunspot group, The location based association is found according to the condition that the distance between a sunspot group detected by ASAP and a solar flare registered by NGDC is less than one 10° radius of corrected the sunspot location as calculated by ASAP.

Furthermore, the difference in time between the detected sunspot group and its associated flare must be less than 6, 12, 24, and 48 h, depending on the forecast lead time window objective.

- X-class flares that are registered without a location in the NGDC catalogue are linked according to time. In this case, if this flare linking with sunspots groups that are found from the same image and same time, only the sunspot group that provides the X-Flarity is evaluated as linked with the reported solar flare.
- The association algorithm updated calculates the values TP, TN, FP, and FN for every single registered in ASAPDATABASE_06, ASAPDATABASE_12, ASAPDATABASE_24, and ASAPDATABASE_48 files according to the following decision thresholds (Table 5):

Table 5. The various thresholds for testing the results of the proposed solar flare prediction system.

Time window	Flarity P_F*(0.9 − 0.1) + 0.1	M flarity P_M*(0.9 − 0.1) + 0.1	X flarity P_X*(0.9 − 0.1) + 0.1
6	0.208	0.431	0.229
12	0.348	0.2291	0.476
24	0.467	0.454	0.53
48	0.695	0.673	0.737

- $P_F = A/(A + NA)$ Percentage of the associated cases to the total number of cases.
- P_M = M and above flares /all cases associated with flares.
- P_X = X flares /all cases associated with flares.

The output of the association algorithm for ASAP system performance is evaluated by applying different measures as explained below.

4.2 Verification the New ASAP's System

The new ASAP system produces forecasts in numerical format, between 0.0 and 1.0, as shown in Table 3. We used different measures for evaluating the forecasts of the new ASAP system. This different measure divided into two types, the first type requires forecast probabilities. So, the system directly converting them to percentages. For instance, if the flaring output of the ASAP system is 0.35, it is supposed that the sunspot group has a 35% flaring probability. On the other hand, the second type of categorical forecasts (Yes/No). The system used a threshold value of 0.5 (50%) for deciding the final forecasts. The first neural network includes output values 0.1 (10%) non-flaring and 0.9 (90%) flaring to sunspot groups. The value of the hybrid system output is determined according to the value of the threshold used if the resulting value is greater than the threshold, there is a possibility of a flare is predicted to occur. Nevertheless, if the value less than the threshold, there is not a possibility of a flare. The second neural network includes two output values. The first output for M-Flare probability and the second output for X-Flare

probability. The M-Flare probability and X-Flare probability are determined according to the value of the threshold used if the resulting value is greater than the threshold, there is a possibility of an M-Flare probability is predicted to occur. However, if the value less than the threshold, there is not a possibility of an M-Flare probability. The same method determines the probability of occurrence X-Flare.

With a view to calculate the success of the produced forecasts the association results are investigated using four criteria are TP, FP, TN, and FN. We referred to these criteria in the previous section. The solar flares in the NGDC catalogues during the verification period (January 1, 2012, to December 31, 2013) are compared with 309535 sunspot groups that were detected from 67,787 MDI image pairs and recorded in ASAPDATABASE_06.txt, ASAPDATABASE_12.txt, ASAPDATABASE_24.txt, and ASAPDATABASE_48.txt for old and new ASAP system. The forecast outputs are compared for different time windows: 6, 12, 24, 48 h. Different prediction verification measures are applied to evaluate our new output system and old ASAP system for each time window as shown in Tables 6 and 7. These measures are arranged in tables as follows (Tables 6 and 7): Probability of Detection (POD), False Alarm Rate (FAR), Percent Correct (PC), Heidke Skill Score (HSS) and Quadratic Score (QR). More details about these measures in a recent paper by [13].

Table 6. Results of the proposed solar flare prediction system.

Time	Type	POD	FAR	PC	QR	HSS
6	Falrity	0.854406	0.499251	0.919021	0.0810	0.63015
	M-flarity	0.738095	0.85514	0.988418	0.0116	0.242014
	X-flarity	0.4	0.9	0.999247	0.0008	0.159978
12	Falrity	0.906371	0.27322	0.868493	0.1315	0.805872
	M-flarity	0.864865	0.614458	0.980164	0.0198	0.533176
	X-flarity	0.5	0.857143	0.998734	0.0013	0.222207
24	Falrity	0.935178	0.076503	0.79621	0.2038	0.928934
	M-flarity	0.888889	0.552795	0.966566	0.0334	0.594895
	X-flarity	0.6	0.769231	0.997706	0.0023	0.333318
48	Falrity	0.942724	0.0417	0.709635	0.2904	0.950158
	M-flarity	0.873239	0.639535	0.946229	0.0538	0.51012
	X-flarity	0.777778	0.5625	0.996265	0.0037	0.559984

POD: the main function of this vector measures the probability of actual solar flares being forecasted true by the ASAP system. The best results for this vector in 48-h time window because the value of this vector is expected that POD would rise with time since there are many significant flares happens in 48-time windows. In new ASAP system for 24 h' time difference POD demonstrates slightly improve in the whole solar flares 93.5%, 88.8% of the M-class flares, and 6.0% of the X-class flares are forecast correctly.

Table 7. Results of the old ASAP system.

Time	Type	POD	FAR	PC	QR	HSS
6	Falrity	0.839884	0.600139	0.937993	2.68E+12	0.535244
	M-flarity	0.531915	0.857143	0.990831	2.68E+12	0.224392
	X-flarity	0.571429	0.973333	0.997467	2.68E+12	0.050773
12	Falrity	0.898763	0.440868	0.906802	2.68E+12	0.683951
	M-flarity	0.625	0.78125	0.985088	2.68E+12	0.323255
	X-flarity	0	1	0.998877	2.68E+12	−4.99E−05
24	Falrity	0.932456	0.280298	0.858383	2.68E+12	0.808277
	M-flarity	0.822917	0.594872	0.975718	2.68E+12	0.542088
	X-flarity	0	1	0.997971	2.68E+12	−5.00E−05
48	Falrity	0.952738	0.188498	0.794965	2.68E+12	0.873182
	M-flarity	0.938967	0.514563	0.961771	2.68E+12	0.638486
	X-flarity	0.916667	0.947494	0.991637	2.68E+12	9.87E−02

Otherwise in old ASAP, the whole solar flares 93.2%, 82.2% of the M-class flares and 0% of the X-class flares.

FAR represents measures the proportion of the ASAP system predicting a solar flare that in effect does not happen. The data shows that FAR produced from new ASAP system improved by a reduced rate of this vector for all time window. False alarm rate has to be reduced in order to improve the reliability of the system.

PC can be defined as a term measure the true forecasts rate of the ASAP system that is the ratio of successful flare and no flare forecasts generated by ASAP system. The data shows that for 24 h' time window difference, 85.8% of whole the forecasts (flare or no flare), 96.6% of M-class forecasts and 99.7% of X-class forecast.

In spite of the fact that PC rates for three-time window are extremely high, that means if the ASAP system supplies just one output, which is no- flare, these PC rates would still be big.

HSS: We have defined this term in the previous part of this report. However, this is a very useful measure when occurrences of the solar flare events to be forecasted very rare. Therefore, HSS is a very significant measure for evaluating forecast of ASAP system. HSS results show that new ASAP forecasts are much more than chance especially for flaring and M-class and X-class flare forecasts. Furthermore, HSS term can be used to optimize the ASAP system by selecting different thresholds value (0.5, 0.45, 0.4, 0.35, and 0.3 were used for our experiences as described earlier).

QR: The quadratic score (QR) represents the mean square error (MSE) of the probabilities provided by the ASAP system. QR is used to calculate the accuracy in probability predictions. In the previous part of this report, we showed the importance of calculating and how to calculate MSE. We compared the results of the new ASAP system with NOAA Space Weather Prediction Centre (SWPC) for the same years from 2012 to 2013

and the 24 h and 48 h prediction results as shown in Table 8. In addition, the average QR (or mean square error) between 2012 and 2013 are also calculated. The results of the comparison showed that ASAP provides better accuracy in predictions than SWPC for M-class and X-class flare predictions.

Table 8. The comparison between the proposed solar flare prediction system with SWPC for QR factor.

Date	Class	24	48
2012–2013 (ASAP)	M	0.0334	0.0538
	X	0.0023	0.0037
2012 (SWPC)	M	0.15	0.15
	X	0.022	0.017
2013	M	0.043	0.12
	X	0.02	0.024
Average	M	0.0965	0.135
	X	0.021	0.0205

5 Conclusions and Future Research

In this paper, we have updated a fully automated hybrid system called Automated Solar Activity Prediction (ASAP) which integrates image processing techniques and machine learning approaches with solar physics. The main aim of this system is predicting automatically whether detected a sunspot group will produce a solar flare and whether this flare will be a C-class, M-class or X-class flare.

The results obtained in this research (HSS, POD, PC, and QR measures) very good compared to the old system, especially when forecasting that a significant solar flare is going to erupt. Particularly, HSS is quite hopeful which displays that new system forecasts are much better than chance. On the other hand, the FAR measure was not good. This is a problem that has to be tackled we are planning to find solutions to this problem in the future. Furthermore, a comparison of QR results of the new system, old ASAP and SWPC showed that the new system provides a better forecast than the ASAP system and SWPC.

Future work will focus on finding solutions to the geometric impact on MDI images near to the limb which considers one of the reasons to changes the classification of sunspot groups that would lead to the wrong prediction. The lack of graphical details for the limb is the major problem blocking us from getting accurate classifications.

References

1. Koskinen, H., et al.: Space weather effects catalogue. ESA Space Weather Study (ESWS) (2001)

2. Pick, M., Lathuillere, C., Lilensten, J.: ESA space weather programme feasibility studies. Alcatel-LPCE Consortium (2001)
3. Lenz, D.: Understanding and predicting space weather. Ind. Phys. **9**(6), 18–21 (2004)
4. Zirin, H., Liggett, M.A.: Delta spots and great flares. Sol. Phys. **113**(1–2), 267–283 (1987)
5. Shi, Z., Wang, J.: Delta-sunspots and X-class flares. Sol. Phys. **149**(1), 105–118 (1994)
6. Raboonik, A., et al.: Prediction of solar flares using unique signatures of magnetic field images. Astrophys. J. **834**(1), 11 (2016)
7. Falconer, D.A., et al.: MAG4 versus alternative techniques for forecasting active region flare productivity. Space Weather **12**(5), 306–317 (2014)
8. Hong, S., et al.: The automatic solar synoptic analyzer and solar wind prediction. In: AGU Fall Meeting Abstracts (2014)
9. Colak, T., Qahwaji, R.: Automated McIntosh-based classification of sunspot groups using MDI images. Sol. Phys. **248**(2), 277–296 (2008)
10. Zell, H.: How SDO Sees the Sun (2017)
11. Qahwaji, R., Colak, T.: Automatic short-term solar flare prediction using machine learning and sunspot associations. Sol. Phys. **241**(1), 195–211 (2007)
12. Fukunaga, R.: Statistical Pattern Recognition. Academic Press, Cambridge (1990)
13. Balch, C.C.: Updated verification of the space weather prediction center's solar energetic particle prediction model. Space Weather **6**(1) (2008)